



**AFRL-RX-WP-TR-2024-0022**



**BIOENGINEERED MICROBIAL SYNTHESIS OF RARE-EARTH  
CONTAINING NANOPARTICLES**

**Nia Oetiker, Blaine Pfeifer, Paras Prasad, and Mark Swihart  
The Research Foundation of State University of New York**

**01 JANUARY 2024  
Final Report**

**DISTRIBUTION STATEMENT A.**

**Approved for public release: distribution is unlimited.**

**AIR FORCE RESEARCH LABORATORY  
MATERIALS AND MANUFACTURING DIRECTORATE  
WRIGHT-PATTERSON AIR FORCE BASE, OH 45433-7750  
AIR FORCE MATERIEL COMMAND  
UNITED STATES AIR FORCE**

## NOTICE AND SIGNATURE PAGE

Using Government drawings, specifications, or other data included in this document for any purpose other than Government procurement does not in any way obligate the U.S. Government. The fact that the Government formulated or supplied the drawings, specifications, or other data does not license the holder or any other person or corporation; or convey any rights or permission to manufacture, use, or sell any patented invention that may relate to them.

This report was cleared for public release by the USAF 88th Air Base Wing (88 ABW) Public Affairs Office (PAO) and is available to the general public, including foreign nationals.

Copies may be obtained from the Defense Technical Information Center (DTIC)  
(<http://discover.dtic.mil>).

AFRL-RX-WP-TR-2024-0022 HAS BEEN REVIEWED AND IS APPROVED FOR PUBLICATION IN ACCORDANCE WITH ASSIGNED DISTRIBUTION STATEMENT.

**DENNIS.PATRICK.BRIAN.1376889099**  
Digitally signed by DENNIS.PATRICK.BRIAN.1376889099  
Date: 2024.04.16 12:12:44 -04'00'

---

PATRICK DENNIS  
Work Unit Manager  
Biomaterials Branch  
Photonic, Electronics & Soft Materials Division

**MEADE.MITCHELL.LEE.1362279409**  
Digitally signed by MEADE.MITCHELL.LEE.1362279409  
Date: 2024.04.16 12:35:16 -04'00'

---

MITCHELL MEADE  
Acting Branch Chief  
Biomaterials Branch  
Photonic, Electronics & Soft Materials Division

This report is published in the interest of scientific and technical information exchange, and its publication does not constitute the Government's approval or disapproval of its ideas or findings.

## REPORT DOCUMENTATION PAGE

<b>1. REPORT DATE</b> 01 January 2024		<b>2. REPORT TYPE</b> Final		<b>3. DATES COVERED</b>	
				<b>START DATE</b> 02 September 2022	<b>END DATE</b> 02 December 2023
<b>4. TITLE AND SUBTITLE</b> Bioengineered Microbial Synthesis of Rare-Earth Containing Nanoparticles for Photon Conversion					
<b>5a. CONTRACT NUMBER</b> FA8650-22-2-7218		<b>5b. GRANT NUMBER</b>		<b>5c. PROGRAM ELEMENT NUMBER</b> 61101E	
<b>5d. PROJECT NUMBER</b> DARPA		<b>5e. TASK NUMBER</b>		<b>5f. WORK UNIT NUMBER</b> X22U	
<b>6. AUTHOR(S)</b> Nia Oetiker, Blaine Pfeifer, Paras Prasad, and Mark Swihart					
<b>7. PERFORMING ORGANIZATION NAME(S) AND ADDRESS(ES)</b> The Research Foundation of State University of New York 402 Crofts Hall Buffalo, NY 14260-0001				<b>8. PERFORMING ORGANIZATION REPORT NUMBER</b> Defense Advanced Research Projects Agency 3701 N Fairfax Drive Arlington VA 22203-1714	
<b>9. SPONSORING/MONITORING AGENCY NAME(S) AND ADDRESS(ES)</b> Air Force Research Laboratory Materials and Manufacturing Directorate Wright-Patterson Air Force Base, OH 45433-7750 Air Force Materiel Command United States Air Force			<b>10. SPONSOR/MONITOR'S ACRONYM(S)</b> AFRL/RXEB	<b>11. SPONSOR/MONITOR'S REPORT NUMBER(S)</b> AFRL-RX-WP-TR-2024-0022	
<b>12. DISTRIBUTION/AVAILABILITY STATEMENT</b> DISTRIBUTION STATEMENT A. Approved for public release: distribution is unlimited.					
<b>13. SUPPLEMENTARY NOTES</b> Report contains color.					
<b>14. ABSTRACT</b> The goal of this study was to develop a bioengineering approach for microbial synthesis of nanoparticles of controlled size and morphology, doped with rare-earth elements (REEs), for application in photon management. The general approach to synthesis of biotic nanomaterials taken in this study is to incubate bacteria with precursors for the desired nanomaterials under conditions that promote bioprecipitation/ biosynthesis of the nanomaterials. This built upon our established capabilities for biosynthesis of metal sulfides, particularly CdS, using both wild-type bacteria and engineered E. coli. Our central hypothesis was that this approach could be adapted, by engineering both the bacteria and the synthesis protocols, to produce rare-earth element (REE) doped nanomaterials under aqueous, near-ambient conditions. Our ultimate target was to dope REEs into fluoride host nanoparticles (prototypically the hexagonal phase of NaYF <sub>4</sub> ) which are the preferred host for REEs in many optical applications. We proposed to test this hypothesis and to progress toward the goal of pure microbial synthesis of REE-doped fluoride nanomaterials in three stages: (i) Dope REEs into CdS by extending existing protocols for CdS biosynthesis; (ii) Biosynthesize the NaYF <sub>4</sub> host phase; and (iii) REEs into fluoride hosts to achieve optical upconversion and downconversion. All of the Bio-INC milestones were achieved. Most importantly, the final project goal of producing ≥2 REE-containing biogenic PCNPs with down conversion quantum.					
<b>15. SUBJECT TERMS</b> Rare Earth Element Doped Nanoparticles, Cadmium Sulfide Quantum Dots, Sodium Yttrium Fluoride Nanoparticles, Fluoroacetate Dehalogenase					
<b>16. SECURITY CLASSIFICATION OF:</b>			<b>17. LIMITATION OF ABSTRACT</b>		<b>18. NUMBER OF PAGES</b> 36
<b>a. REPORT</b> Unclassified	<b>b. ABSTRACT</b> Unclassified	<b>c. THIS PAGE</b> Unclassified	SAR		
<b>19a. NAME OF RESPONSIBLE PERSON</b> Patrick Dennis				<b>19b. PHONE NUMBER (Include area code)</b> (937) 255-9068	

Distribution Statement A. Approved for public release: distribution is unlimited.

## Table of Contents

Section	Page
List of Figures.....	ii
List of Tables .....	iv
1. Summary.....	1
2. Introduction.....	3
3. Methods, Assumptions, and Procedures.....	6
4. Results and Discussion.....	8
4.1 Task 1: Doping CdS NPs with REEs in <i>E. coli</i> .....	8
4.2 Task 2: Biosynthesis of REE-doped NaYF <sub>4</sub> NPs in <i>E. coli</i> .....	9
4.3 Task 3. Engineer rational control of PNCP biosynthesis and properties .....	15
4.4 Task 4. Produce and optimize more complex REE-containing NPs in <i>E. coli</i> .....	17
5. Conclusion .....	19
6. References .....	20
Appendix 1. Project Coordination, Dissemination, and Translation Efforts .....	25
Appendix 2. Schedule: Milestones and Deliverables .....	27
LIST OF SYMBOLS, ABBREVIATIONS, AND ACRONYMS.....	30

## List of Figures

Figure	Page
Figure 1. Summary of evidence satisfying Month 2 milestone. ....	8
Figure 2. Absorbance and emission spectra showing that biosynthesized Er-doped CdS met month 3 milestone. ....	9
Figure 3. Transmission electron microscopy, elemental analysis, and fluorescence emission analysis of UCNPs biosynthesized by <i>S. baltica</i> . A) HAADF image from nanoparticles adhered to the outer cell membrane and extracellular region (white arrow). B) EDS of these elements, mapping sodium (yellow), fluorine (green), yttrium (red), ytterbium (purple), and erbium (white) elemental maps. C) Confocal microscopy analysis of cells from UCNP biosynthesis using <i>S. baltica</i> stained with DAPI, 980 nm excited upconverted emission from cells, and merged image. ....	10
Figure 4. Representative XRD patterns from UCNPs biosynthesized using genetically modified <i>E. coli</i> and optical emission spectra observed upon exciting the UCNPs with a 980 nm laser. ....	11
Figure 5. Size analysis of UCNPs produced by <i>S. baltica</i> after different times of heating at 200 °C. (A) TEM image and (B) size distribution of concentrated UCNPs from the supernatant without post-biosynthesis heating. The sizes of the NPs range from 30 to 70 nm. (C) TEM image and (D) size distribution of UCNPs heated at 200°C for 1 h. The size range of the NPs is mainly between 4 to 7 nm. (E) TEM image and (F) size distribution of UCNPs heated at 200°C for 24 h. The NP size range is between 5 and 10 nm. ....	12
Figure 6. TEM size analysis from UCNPs synthesized in room temperature protocol using genetically modified <i>E. coli</i> $\Delta crcB$ , $\Delta crcB$ LanM and $\Delta crcB$ LanM-LutH cells. ....	13
Figure 7. Transmission electron microscopy characterization of purified TbS NPs produced by <i>E. coli</i> . (A) TEM micrograph of purified TbS NPs. (B) Size frequency distribution of purified NPs. (C, D, E) High resolution TEM micrographs of the biosynthesized TbS NPs. The inset in Figure E shows the selected area electron diffraction pattern obtained in the TEM. (E) STEM-HAADF image and the corresponding EDS elemental maps showing (G) sulfur and (H) terbium localization. ....	14
Figure 8. TEM images, selected area electron diffraction pattern, and particle size distribution from image analysis for biosynthesized yttrium sulfide NPs. ....	15
Figure 9. Schematic illustration of strategies employed for genetic modification of <i>E. coli</i> . ....	15
Figure 10. Illustration of methodology used to introduce metal-binding protein expression and summary list of plasmids and proteins expressed in <i>E. coli</i> for this project. ....	16
Figure 11. TEM images of chemically synthesized NaYF <sub>4</sub> NPs. A) cubic and B) hexagonal phase NaYF <sub>4</sub> . C) High resolution TEM image of hexagonal NaYF <sub>4</sub> NPs. XRD patterns of D) cubic phase and E) hexagonal phase NaYF <sub>4</sub> NPs. Sharp impurity peaks are salt (NaCl) residue. ....	17
Figure 12. Representative TEM images of TbS core/Ys shell nanoparticles. ....	18

Figure 13. Illustration of integrating sphere configuration used for measurement of quantum yield (QY) of downconverted emission from 390 nm to the wavelengths indicated in the energy level diagram. As tabulated in the accompanying table, the QY of TbS emission was dramatically enhanced by doping with Gd and by coating with an yttrium-rich shell. .... 18

## List of Tables

<b>Table</b>	<b>Page</b>
Table 2-1. Summary of Tasks and Completion Dates	27

## 1. Summary

The goal of this study was to develop a bioengineering approach for microbial synthesis of nanoparticles of controlled size and morphology, doped with rare-earth elements (REEs), for application in photon management. The general approach to synthesis of biotic nanomaterials taken in this study is to incubate bacteria with precursors for the desired nanomaterials under conditions that promote bioprecipitation/ biosynthesis of the nanomaterials. This built upon our established capabilities for biosynthesis of metal sulfides, particularly CdS, using both wild-type bacteria and engineered *E. coli*. Our central hypothesis was that this approach could be adapted, by engineering both the bacteria and the synthesis protocols, to produce rare-earth element (REE) doped nanomaterials under aqueous, near-ambient conditions. Our ultimate target was to dope REEs into fluoride host nanoparticles (prototypically the hexagonal phase of NaYF<sub>4</sub>) which are the preferred host for REEs in many optical applications. We proposed to test this hypothesis and to progress toward the goal of pure microbial synthesis of REE-doped fluoride nanomaterials in three stages: (i) Dope REEs into CdS by extending existing protocols for CdS biosynthesis; (ii) Biosynthesize the NaYF<sub>4</sub> host phase; and (iii) REEs into fluoride hosts to achieve optical upconversion and downconversion. Key outcomes and accomplishments of this study can be summarized as follows:

- Demonstrated the first strictly microbial, aqueous and near-ambient temperature biosynthesis of REE-based nanoparticles exhibiting upconversion, by identifying a novel fluoride-tolerant extremophile (*Shewanella baltica*) with inorganic biosynthesis ability.
- Demonstrated, in groundbreaking research, the strictly microbial biosynthesis of fluoride-based nanoparticles. This answered the open question of whether fluoride-containing particles could be produced, given the very limited role of fluorine in biological systems (compared, for example to sulfur) and the lack of any prior studies of biosynthesis of fluoride phases.
- Produced, for the first time, under aqueous near-ambient conditions, rare-earth sulfides (TbS, EuS) that are not readily prepared by chemical methods. This demonstrates a new capability of biosynthesis with clear advantages over chemical synthesis.
- Demonstrated the first biosynthesis of upconverting rare-earth fluoride particles using *E. coli* genetically modified to overexpress specific metal-binding proteins. This is a key step toward harnessing our bioengineering capabilities to rationally design organisms for biosynthesis. Clear effects of genetic modification, including enhanced localization of REE in the periplasmic space, were observed.
- Tested and built understanding of different intracellular and extracellular routes of REE-based nanoparticle formation, producing fundamental insights into particle formation mechanisms.
- Demonstrated REE NP formation from two biological host systems, *Shewanella baltica* (an extremophile with innate inorganic NP formation ability) and *E. coli* (a model bacterium for cellular engineering). Each opens multiple future directions for biogenic REE NP production.

- Produced the first demonstration of the use of bacteria in room-temperature aqueous chemical synthesis of REE-doped NaYF<sub>4</sub>, achieving bright upconversion and showing the ability to alter optical properties using *E. coli* in place of a traditional reagent.

Ultimately, these outcomes suggest several promising new research directions that could fruitfully be pursued in subsequent research. The opportunity with the most immediate promise is the microbial synthesis of rare-earth sulfides, which are difficult to synthesize by conventional chemical routes, and which are therefore an underexplored but promising family of semiconductors. In the longer term, large-scale genetic modification of *E. coli* to enhance its ability to produce the rare earth fluorides could pay dividends both in terms of intentional nanoparticle synthesis, and also for capture and separation of rare-earth elements.

## 2. Introduction

Lanthanide-doped upconversion nanoparticles (UCNPs) represent a highly promising advancement in the realm of bioimaging agents. Through a process known as upconversion (UC), these nanoparticles (NPs) harness the sequential absorption of multiple photons by leveraging the extended lifetime and intricately structured energy levels of trivalent lanthanide ions within a tailored inorganic host lattice. UCNPs are versatile tools for various bioimaging applications, promising enhanced depth penetration and resolution for imaging biological structures and processes.<sup>1,2</sup> Typically, UCNPs consist of a matrix, sensitizer, and activator, although some singly-doped UCNPs may lack the sensitizer component. The matrix plays a central role in determining UCNP properties, with  $\text{Y}^{3+}$ ,  $\text{La}^{3+}$ , and  $\text{Lu}^{3+}$  ions being commonly used. Activators, such as  $\text{Pr}^{3+}$ ,  $\text{Nd}^{3+}$ ,  $\text{Sm}^{3+}$ ,  $\text{Tb}^{3+}$ ,  $\text{Ho}^{3+}$ ,  $\text{Er}^{3+}$ , and  $\text{Tm}^{3+}$  are incorporated into the matrix as luminescence centers. To enhance luminescence efficiency, another rare-earth ion, typically  $\text{Yb}^{3+}$ , can be incorporated as a sensitizer.<sup>3</sup>

$\text{NaYF}_4:\text{Yb,Er}$  is widely recognized as one of the most efficient compositions for UCNPs.<sup>4</sup> Upon excitation by a 980 nm near-infrared (NIR) laser, the electrons in  $\text{Yb}^{3+}$  within  $\text{NaYF}_4:\text{Yb,Er}$  NPs are initially excited. After that, two consecutive energy-transfer processes excite an  $\text{Er}^{3+}$  ion to a high excited state. Subsequently, after one or more nonradiative decay steps  $\text{Er}^{3+}$  can emit a visible photon (red or green).<sup>5,6</sup>

These NPs offer an intriguing alternative to conventional fluorescent probes like organic dyes and quantum dots. While traditional probes may boast high quantum yields, they often face limitations such as photodegradation, erratic switching between bright emission and darkness, low tissue penetration of UV light needed for excitation, and poor biocompatibility.<sup>7</sup> In contrast,  $\text{NaYF}_4$  NPs doped with  $\text{Er}^{3+}$  and  $\text{Yb}^{3+}$  exhibit several advantageous properties, including strong up-converted luminescence, narrow luminescence peaks, low background emission, long fluorescence lifetimes, resistance to blinking, and good biocompatibility.<sup>8</sup>

Moreover, REE-doped  $\text{NaYF}_4$  NPs are excited using near-infrared light, which boasts superior tissue penetration due to lower absorption compared to UV and visible light and generates no autofluorescence.<sup>9</sup> These exceptional properties have garnered significant interest for a wide range of applications, including super-resolution microscopy,<sup>10</sup> augmenting solar cell efficiency,<sup>11</sup> latent fingerprint detection,<sup>12</sup> optogenetics,<sup>13,14</sup> photodynamic therapy,<sup>15</sup> and sensing.<sup>16</sup>

Presently, the synthesis of  $\text{NaYF}_4:\text{Yb,Er}$  NPs is primarily achieved through chemical processes, including thermal decomposition (involving organometallic precursors heated in organic solvents), hydrothermal/solvothermal synthesis (in which rare-earth elements, water, or organic solvents are heated under high pressure), and co-precipitation (a conventional method for synthesizing inorganic NPs that typically involves the use of surfactants).<sup>17</sup> However, conventional chemical synthesis methods for producing UCNPs pose risks due to the potential presence of toxic chemical species adsorbed on the surface of NPs, thereby limiting their suitability for medical applications.<sup>18</sup>

In light of the limitations and drawbacks associated with conventional physical and chemical methods of nanoparticle (NP) synthesis, researchers have increasingly turned to biological

systems as viable alternatives. Microorganisms, in particular, have emerged as environmentally-friendly "factories" for NP synthesis.<sup>19</sup> Unlike traditional methods, biological synthesis harnesses the innate mechanisms of living organisms to condense potentially toxic metal species into NPs.

Utilizing biological catalysts inherently requires lower temperatures and pressures, and eliminates the need for toxic reagents or solvents. Furthermore, the resulting NPs often exhibit reduced cytotoxicity and phytotoxicity, rendering them suitable for various biomedical applications.<sup>20</sup> Algae, plants, yeasts, and bacteria are among the diverse range of biological agents capable of performing NP biosynthesis, each contributing to the production of distinct types of NPs. This diversity in biological systems yields a wide array of NP shapes, sizes, compositions, and surface state, expanding the range of properties and potential applications of these NPs.<sup>21</sup>

The genus *Shewanella* exhibits remarkable capabilities in reducing a wide range of metal species, leading to the biomineralization of diverse metal NPs. Molecular mechanisms associated with *Shewanella* for NPs biosynthesis have been extensively documented.<sup>22</sup> While the use of microorganisms for synthesizing NPs is well-established, exploring their potential for synthesizing UCNPs is a new and essentially unexplored direction.

Recent studies have highlighted the ability of *Shewanella oneidensis* MR-12 to absorb REEs, laying the groundwork for investigating their role in UCNP biosynthesis.<sup>23,24</sup> Moreover, screenings of *Shewanella oneidensis* MR-12 knock-out strains have demonstrated their capability to remove a mixture of REEs from aqueous solution, including ytterbium (Yb), a crucial sensitizer in UCNPs.<sup>25</sup>

Given these emerging properties, we tested the *Shewanella* genus as a biofactory to UCNP biosynthesis through an easy low temperature and low precursors concentration protocol. Specifically, we selected *Shewanella baltica*, isolated from the Antarctic region, renowned for its resistance to cadmium and tellurium and its ability to biosynthesize cadmium sulfide (CdS) quantum dots.<sup>26,27</sup> The positive outcomes reported in this study represent a pioneering example of UCNP synthesis through bacterial biosynthesis.

Lanthanide (Ln<sup>3+</sup>)-based NPs are employed in numerous technologies including radar, computer screens, drug-delivery systems, and high penetration bioimaging.<sup>[28-30]</sup> Many of these applications are based on their photoluminescence. Lanthanides with the most efficient downconverting visible luminescence include trivalent terbium, europium (Eu), and samarium (Sm) ions.<sup>[31]</sup> Their temporal and spectral properties (long lifetime, sharp emission bands, and large Stokes shifts) make them particularly useful in time-resolved luminescence bioassays. Their emission is easily distinguished from autofluorescence based on its much longer lifetime.<sup>[32]</sup> Although Tb is one of the most luminescent lanthanides, reports of synthesis of Tb-based NPs are rare.

NPs are commonly made through chemical synthesis, but the large solvent volumes and high temperatures needed for this approach often limit large scale application. Thus, green and more sustainable processes to synthesize Tb-containing NPs using biological systems at low temperature without toxic reagents or solvents are needed. A few methods to produce Tb-containing NPs have been reported, mostly based on chemical synthesis.<sup>[33-35]</sup>

Metal sulfide NPs (MeS NPs) are used in applications such as antibacterial agents, imaging and diagnostics, photo- and chemotherapy, pharmacology, and the manufacture of biosensors.<sup>[36]</sup> Many Me-S NPs are biocompatible and exhibit physicochemical properties that are useful for biological applications.<sup>[37]</sup> Chitosan-capped TbS (CS-Tb<sub>2</sub>S<sub>3</sub>) NPs produced using a bottom-up chemical method were recently reported.<sup>[33]</sup> Chemical synthesis of REE-doped NPs of metal sulfides including CdS, ZnS, and PbS has been reported in several studies.<sup>[38–42]</sup> These REE-doped NPs form a new class of luminescent materials with narrow emission lines, a large separation between the excitation and emission wavelengths, and a long emission lifetime.<sup>[43]</sup> Thus, sulfide lattices have potential to be good hosts for Tb.

Studies of the interaction of REEs with cells or biomolecules have, to date, been limited. Some specific enzymes that interact and bind Ln<sup>3+</sup> ions have been described. In this context, the identification, molecular structure, and nucleotide sequence of a Ce<sup>3+</sup>-induced methanol dehydrogenase (MDH) from *Bradyrhizobium* sp.<sup>[44]</sup> and the induction of MDH activity by La<sup>3+</sup> ions on proteins exhibiting MDH activity in *Methylobacterium radiotolerans*<sup>[45]</sup> were reported. Later, the MDH gene homologue, *xoxF1*, was shown to be upregulated in response to La<sup>3+</sup> exposure in *Methylobacterium extorquens*.<sup>[46]</sup> A highly selective Ln<sup>3+</sup>-binding protein called lanmodulin (LanM) was identified in *M. extorquens*.<sup>[47]</sup> Despite these prior reports, the biological relevance of lanthanides remains unknown, and studies of their interactions with cells are needed.

Tb compounds are considered to be of low to moderate toxicity, but only a few reports about Tb interaction with biological systems have been published.<sup>[48–50]</sup> The minimal inhibitory concentrations of different Tb compounds against pathogenic bacteria have been described, with *Pseudomonas aeruginosa*, *Escherichia coli*, and *Staphylococcus aureus* showing MICs over 1 mM.<sup>[51]</sup> Tb biosorption and selectivity by a genetically modified *E. coli* strain expressing lanthanide binding tags on the cell surface has been reported.<sup>[52,53]</sup> Just one study reporting the biological synthesis of Tb<sub>2</sub>O<sub>3</sub> NPs, by incubating Tb<sub>4</sub>O<sub>7</sub> with *Fusarium oxysporum* biomass has been published. *F. oxysporum* produces compounds with a very high reduction potential, which can reduce Tb<sub>4</sub>O<sub>7</sub> in aqueous media, yielding Tb<sub>2</sub>O<sub>3</sub> NPs with a 10 nm size.<sup>[54]</sup>

### 3. Methods, Assumptions, and Procedures

The general approach to synthesis of biotic nanomaterials taken in this study is to incubate bacteria with precursors for the desired nanomaterials under conditions that promote bioprecipitation/ biosynthesis of the nanomaterials. This built upon our established capabilities for biosynthesis of metal sulfides, particularly CdS, using both wild-type bacteria and engineered *E. coli*. Our central hypothesis was that this approach could be adapted, by engineering both the bacteria and the synthesis protocols, to produce rare-earth element (REE) doped nanomaterials under aqueous, near-ambient conditions. Our ultimate target was to dope REEs into fluoride host nanoparticles (prototypically the hexagonal phase of NaYF<sub>4</sub>) which are the preferred host for REEs in many optical applications. We proposed to test this hypothesis and to progress toward the goal of pure microbial synthesis of REE-doped fluoride nanomaterials in three stages:

(i) **Dope REEs into CdS by extending existing protocols for CdS biosynthesis.** Here, our approach was to add REE precursors to our existing protocols for CdS biosynthesis, for multiple bacterial strains, to test whether the cells would tolerate the REEs, whether the cells would precipitate the REEs, and whether the REEs would be incorporated into the CdS nanoparticles. Finally, we would test whether the CdS host material could serve as a photosensitizer for the REEs. CdS nanoparticles exhibit strong, size-dependent absorbance and could potentially transfer energy to REEs, which would then re-emit with their characteristic narrow emission spectrum at much longer wavelengths. We proposed to begin this work with Er<sup>3+</sup> doping of CdS. Doping of REEs into CdS is inherently challenging because the REEs prefer to be in a +3 oxidation state, rather than the +2 oxidation state of Cd in CdS, and the REEs are relatively “hard” acids, in the context of hard-soft acid-base theory, and thus interact more strongly with hard bases (O<sup>2-</sup>, F<sup>-</sup>) than soft bases (S<sup>2-</sup>). While this approach is challenging, it is lower-risk than the synthesis of the fluoride-doped particles and thus provides a risk-mitigation strategy for the overall project.

(ii) **Biosynthesize the NaYF<sub>4</sub> host phase.** Here, our aim was to use fluoride-tolerant or fluoride-producing bacteria to promote fluoride accumulation within the cell. Although we initially proposed exploring the expression of dehalogenase enzymes to release intracellular F<sup>-</sup>, we quickly determined that the toxicity of the intended fluoroacetate precursors would be an impediment to this path and that some fluoride-resistant and fluoride accumulating strains were already available. Thus, we focused on employing these strains to generate the fluoride-containing host nanoparticles. We note that there were no prior reports of the microbial biosynthesis of REE-doped fluorides in the literature, and thus the pursuit of this host phase was a high-risk, high-reward undertaking.

(iii) **Incorporate REEs into fluoride hosts to achieve optical upconversion and downconversion.** Finally, our plan was to combine learnings from the prior two steps to produce the first microbial biosynthesized REE-doped fluoride nanoparticles and characterize their physicochemical and optical properties. As a general approach for biosynthesis of REE-doped NPs, we aimed to co-express multiple genes, each with the prospect of contributing to NP formation, using plasmids designed to overexpress multiple genes in different combinations to evaluate their effects on NP production. In this context, we planned to express proteins, peptides,

and small biomolecules favoring the binding of the REIs of interest for template-assisted growth (e.g., metallophores, phytochelatins, metallothioneins, and glutathione). Here, the intent was to induce controlled biosynthesis of NPs by binding individual ions or clusters of  $Y^{3+}$  and REE ions for reaction with  $F^-$  to initiate NP nucleation.

The first REE to be employed in these studies was erbium, based on its ability to both upconvert (to visible wavelengths) and downconvert (to  $\sim 1550$  nm, “communications” wavelengths) from near infrared light at 800 or 980 nm. The second REE of interest was ytterbium, due to its ability to serve as a sensitizer for erbium, based on its relatively strong absorbance near 980 nm. Energy transfer from  $Yb^{3+}$  to  $Er^{3+}$  followed by upconverted emission provides clear evidence of co-incorporation of erbium and ytterbium into the same nanoparticles. Other emitters of interest were thulium, based on its ability to downconvert from 800 nm to  $\sim 1650$  nm, and terbium, based on both its inherent emission and its ability to sensitize erbium. Several other rare-earth ions including gadolinium and europium were also of interest for downconversion at visible wavelengths.

We also proposed synthesis of REE-doped materials by conventional chemical routes, for benchmarking, and characterization of both biosynthesized and chemically synthesized nanomaterials by an array of methods including electron microscopy, x-ray diffraction, Raman spectroscopy, absorbance and photoluminescence spectroscopy, and other means.

Further details of experimental protocols are provided in the subsequent section, adjacent to the results of those protocols.

## 4. Results and Discussion

In this section, based on the very specific tasks and milestones of the project, we present the results and discussion in terms of those milestones, in chronological order. The first milestone was at the end of the 2<sup>nd</sup> month of the project.

### 4.1 Task 1: Doping CdS NPs with REEs in *E. coli*.

**Month 2 Milestone:** Demonstrate the ability to use a bioengineering approach to change the identity of specific REE incorporated within the structure of a biosynthesized inorganic nanoparticle for  $\geq 2$  different REEs.

To biosynthesize CdS NPs, the bacterial suspension was supplemented with 1 mM L-cysteine and 100  $\mu$ M CdCl<sub>2</sub>, then the suspension was incubated with agitation at 37 °C for one hour. To synthesize the REE-doped CdS NPs, the same protocol was followed, and the doping agent (REE nitrate) was added. Erbium (Er<sup>3+</sup>), ytterbium (Yb<sup>3+</sup>), terbium (Tb<sup>3+</sup>), neodymium (Nd<sup>3+</sup>), gadolinium (Gd<sup>3+</sup>) and europium (Eu<sup>3+</sup>) nitrate doping were evaluated. Figure 1 demonstrates achievement of this milestone, specifically showing incorporation of Nd and Er into CdS.

#### REE-doped CdS nanoparticles met month 2 milestone

- Extended known method for extracellular synthesis of CdS quantum dots to incorporate rare-earth elements
- Controls show no nanoparticle formation without live bacteria (*e.g.*, medium only, dead cells, cell extract)
- EDS mapping directly demonstrated incorporation of Nd and Er into CdS by biosynthesis

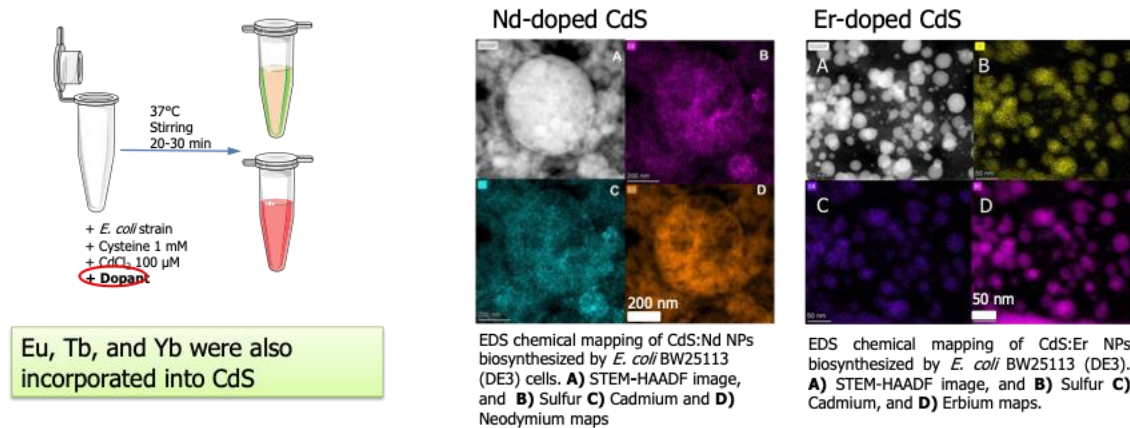


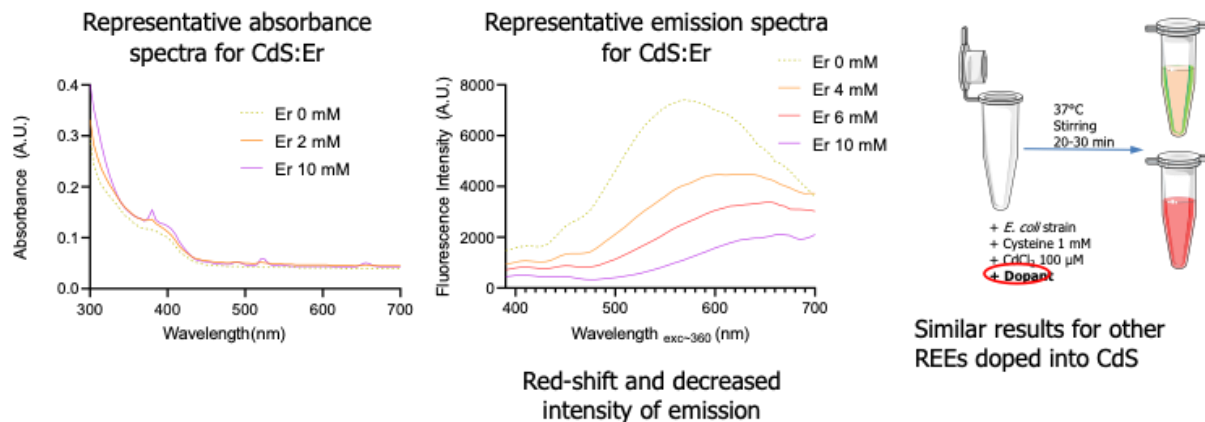
**Figure 1. Summary of evidence satisfying Month 2 milestone.**

**Month 3 Milestone (Optical):** Engineer a biological system to produce, and then test, functional REE-containing nanoparticles: Demonstrate a single biogenic nanoparticle composition that absorbs and emits light in the visible (400 – 700 nm) or near-IR (NIR, 700 nm – 1500 nm) with an upconverting or down-converting mechanism.

The absorbance and emission spectra of CdS:Er in Figure 2 demonstrate achievement of this milestone. However, as noted, we did not see evidence of energy transfer from CdS to the REE dopants, or emission from the REEs.

All REE-doped CdS nanoparticles exhibit CdS-like downconversion, which is modified by incorporation of REEs

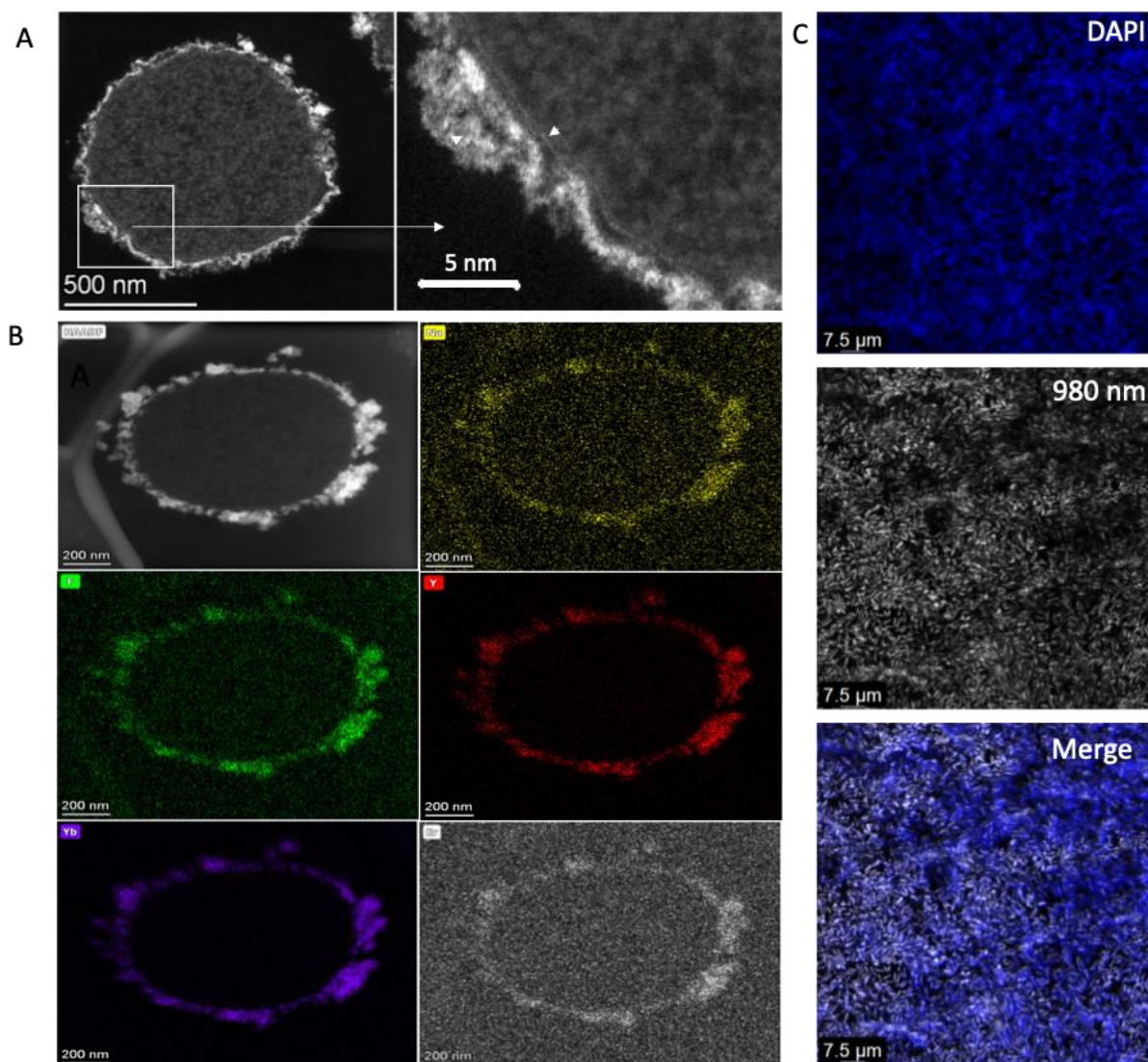
Technically **met month 3 milestone**, but no evidence of energy transfer from CdS to REEs (CdS-sensitized REE emission)



**Figure 2. Absorbance and emission spectra showing that biosynthesized Er-doped CdS met month 3 milestone.**

#### 4.2 Task 2: Biosynthesis of REE-doped NaYF<sub>4</sub> NPs in *E. coli*

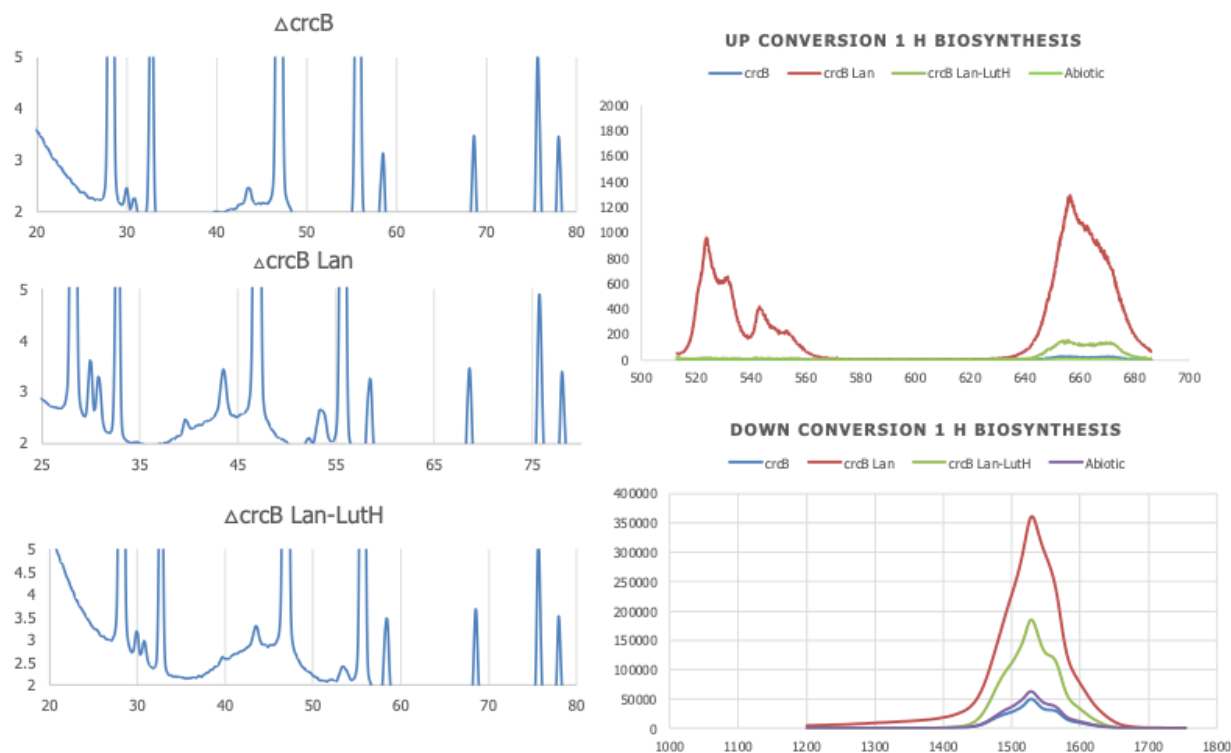
In our initial experiments with *E. coli*, we observed nanoparticle formation but did not achieve the upconverted emission that is characteristic of NaYF<sub>4</sub> co-doped with Yb<sup>3+</sup> and Er<sup>3+</sup>. Thus, in parallel with efforts to genetically engineer *E. coli*, we analyzed the capacity of an extremophile that is highly resistant to fluoride ions to generate upconverting REE-doped nanoparticles in the presence of low concentrations of precursors. For that, we incubated *Shewanella baltica* cells in presence of 0.5 mM of NaF, Y(NO<sub>3</sub>)<sub>3</sub>, Yb(NO<sub>3</sub>)<sub>3</sub> and 0.001 mM of Er(NO<sub>3</sub>)<sub>3</sub> in weakly acidic buffer for 1 h. Cells were then washed and the UCNPs presence was analyzed. We could detect the presence of electron-dense nanostructures in the periplasmatic and extracellular space and adhered to outer cell membrane (Figure 3A). These NPs were composed of Na, Y, F, Yb and Er (Figure 3B). When we excited washed cells after biosynthesis at 980 nm (Figure 3C), we could detect emission from cells (DAPI and 980 nm emission merge image). This emission was detected with a peak at 540 nm showing the characteristic upconverted green emission from Yb<sup>3+</sup> sensitized Er<sup>3+</sup>.



**Figure 3. Transmission electron microscopy, elemental analysis, and fluorescence emission analysis of UCNPs biosynthesized by *S. baltica*. A) HAADF image from nanoparticles adhered to the outer cell membrane and extracellular region (white arrow). B) EDS of these elements, mapping sodium (yellow), fluorine (green), yttrium (red), ytterbium (purple), and erbium (white) elemental maps. C) Confocal microscopy analysis of cells from UCNPs biosynthesis using *S. baltica* stained with DAPI, 980 nm excited upconverted emission from cells, and merged image.**

**TASK 2.2: Synthesize NaYF<sub>4</sub> NPs in recombinant *E. coli* strain:** We developed genetically modified bacteria *E. coli*  $\Delta$ *crcB* (hyperaccumulator of fluoride),  $\Delta$ *crcB*-LanM (hyperaccumulator of fluoride and REE),  $\Delta$ *crcB*-LanM-LutH (hyperaccumulator of fluoride and REE). We designed a protocol at room temperature, with genetically modified bacteria added in the absence of organic solvents at room temperature, where the obtained NaYF<sub>4</sub>Yb:Er nanoparticles emitted at

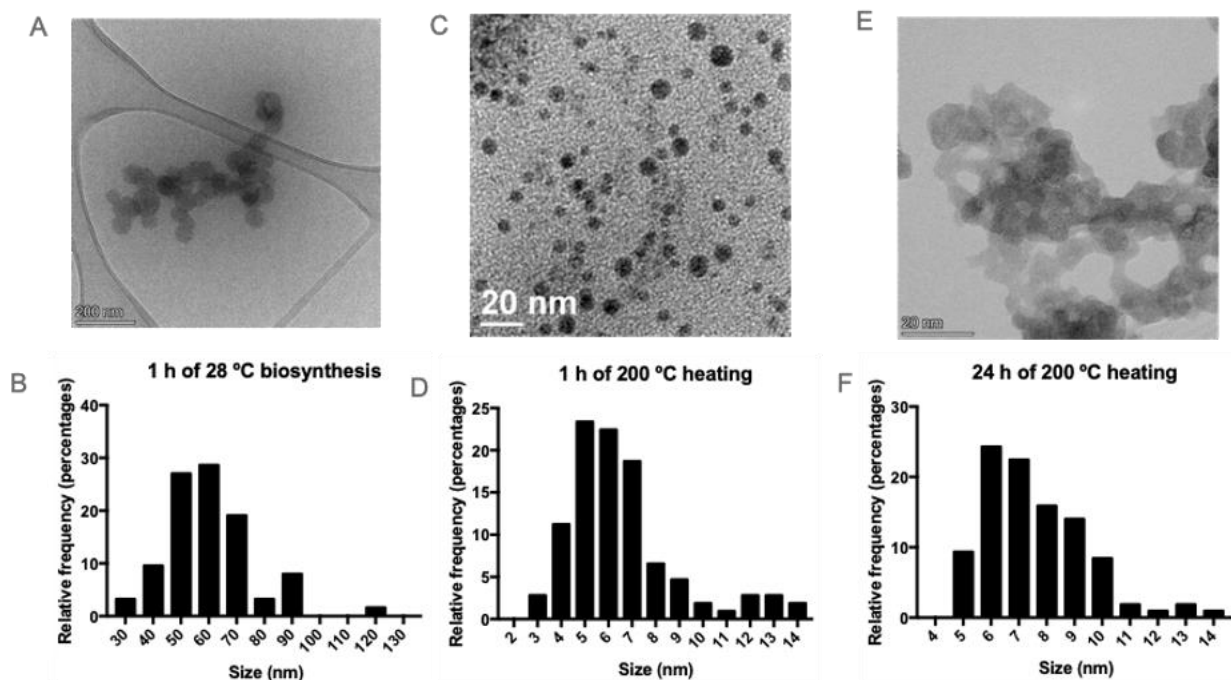
520-520 nm and 650 nm (upconversion) and 1550 nm (downconversion) when excited at 980 nm (Figure 4).



**Figure 4. Representative XRD patterns from UCNPs biosynthesized using genetically modified *E. coli* and optical emission spectra observed upon exciting the UCNPs with a 980 nm laser.**

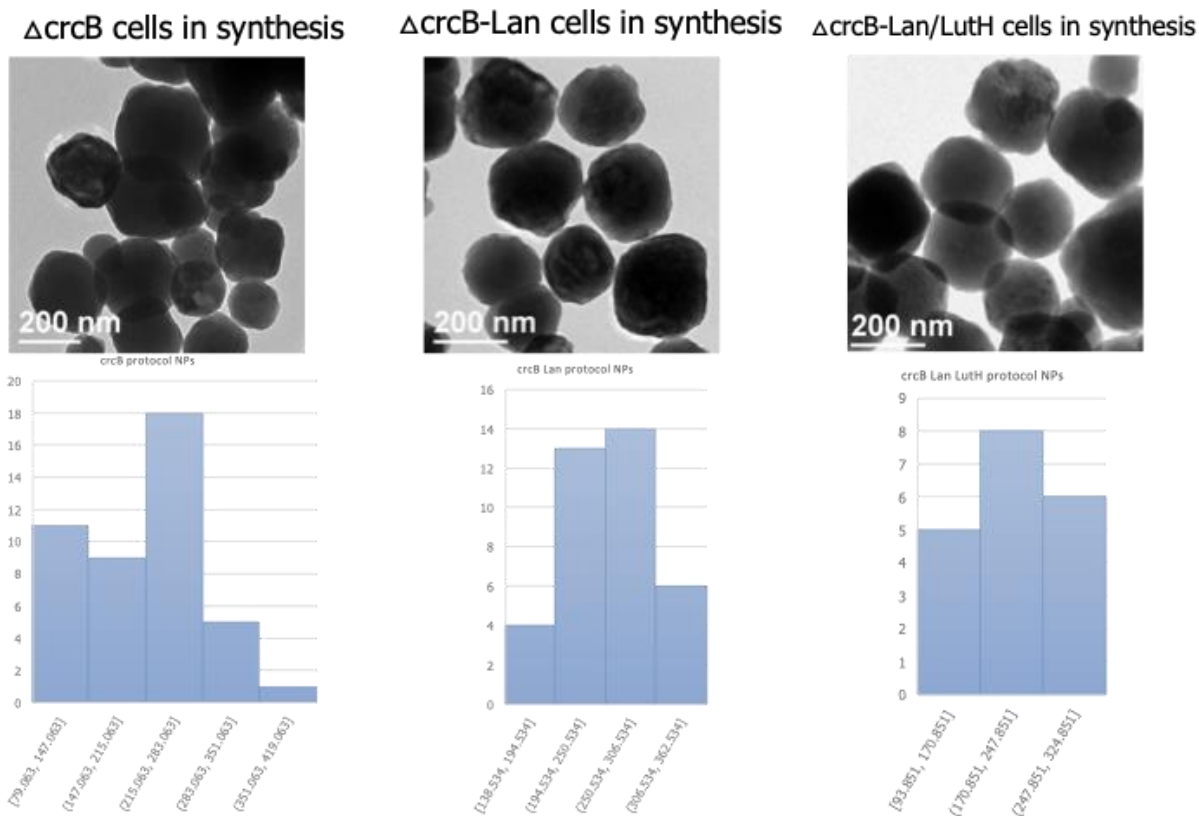
### MILESTONE 3: Bio-based production of similarly sized nanoparticles (50 nm width)

We developed different size REE doped NPs from each treatment. From the low concentration biosynthesis process in *Shewanella baltica*, after 1 h of incubation at 28 °C we detected a size range from 30 at 90 nm (Figure 5A,B). Post-biosynthesis heat treatment, conducted at 200°C for either 1 hour (Figure 5C,D) or 24 hours (Figure 5E,F) in an unstirred autoclave reactor within an oven, improved the up-conversion emission of these NPs. Despite not reaching the temperature threshold required for complete organic matter removal via carbonization (*i.e.*, at least 350°C for 16 hours), we believe the post-biosynthesis heat treatment will reduce the influence of biomolecules associated with the NPs, which may otherwise negatively impact optical properties, and enhance the crystallinity of NPs, which can enhance upconverted emission. These heated UCNPs have a ranged size between 3-10 nm and are stable at temperature.



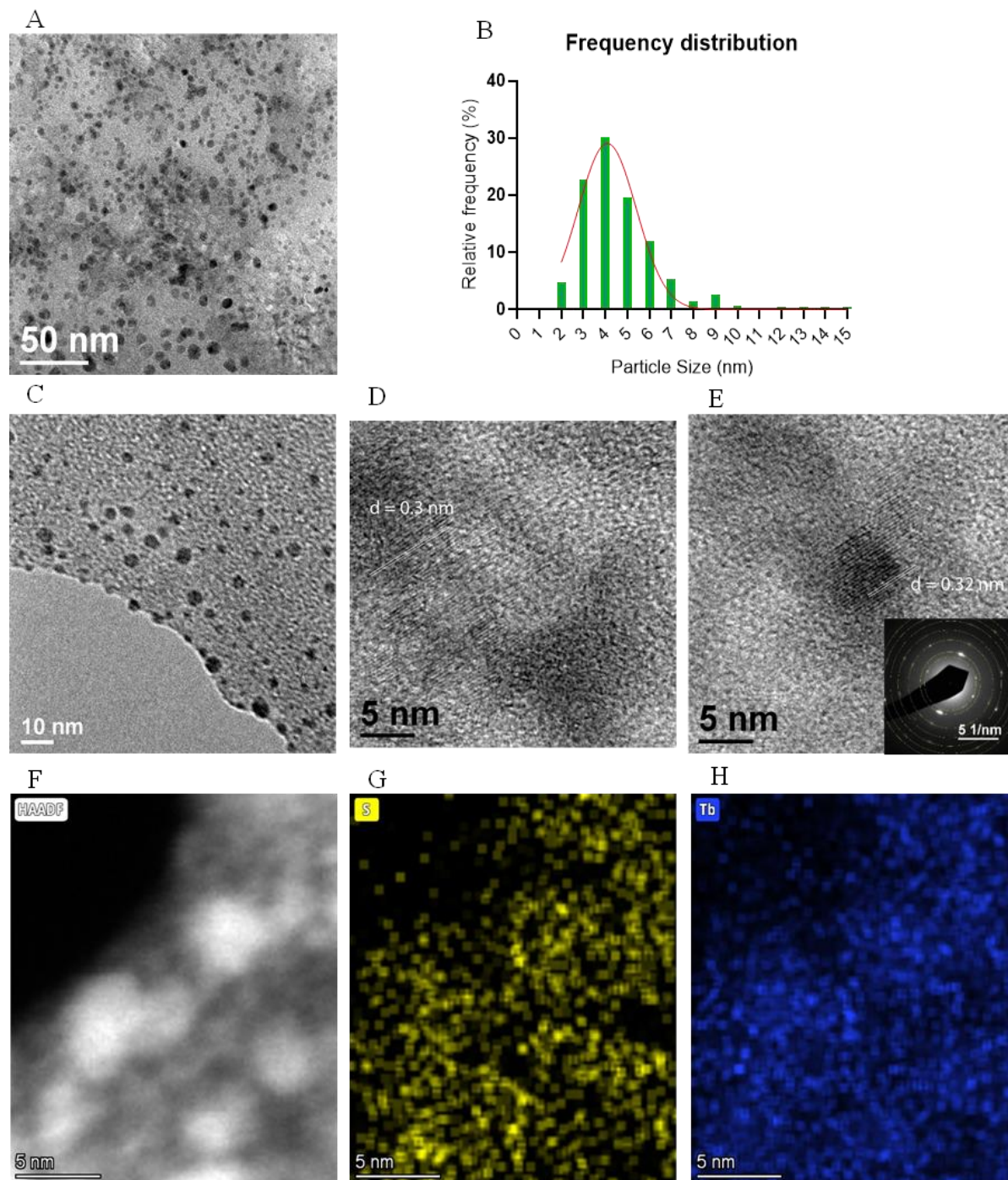
**Figure 5. Size analysis of UCNPs produced by *S. baltica* after different times of heating at 200 °C. (A) TEM image and (B) size distribution of concentrated UCNPs from the supernatant without post-biosynthesis heating. The sizes of the NPs range from 30 to 70 nm. (C) TEM image and (D) size distribution of UCNPs heated at 200°C for 1 h. The size range of the NPs is mainly between 4 to 7 nm. (E) TEM image and (F) size distribution of UCNPs heated at 200°C for 24 h. The NP size range is between 5 and 10 nm.**

On the other hand, from a room temperature high concentration protocol we developed NPs very similar in size. The size of NaYF<sub>4</sub>:Yb:Er NPs made with genetically modified *E. coli* ranged from 70-280 nm in  $\Delta crcB$  cells, 138-300 nm in  $\Delta crcB$  LanM and 90-250 nm in  $\Delta crcB$  LanM-LutH cells (Figure 6).



**Figure 6. TEM size analysis from UCNPs synthesized in room temperature protocol using genetically modified *E. coli*  $\Delta$ *crcB*,  $\Delta$ *crcB* LanM and  $\Delta$ *crcB* LanM-LutH cells.**

Moreover, we obtained  $Tb_2S_3$  (Figure 7) and  $Y_2S_3$  NPs by adapting a protocol for extracellular synthesis of other metal sulfides, with REE precursors. Crystalline nanoparticles were produced at ambient conditions using unmodified *E. coli*. Terbium was the first REE selected for this approach, based on its readily observed visible downconversion under UV excitation. These NPs ranged in size from 2-7 nm. In addition to terbium sulfide and yttrium sulfide, we have produced similar sulfides of erbium, europium, and ytterbium.



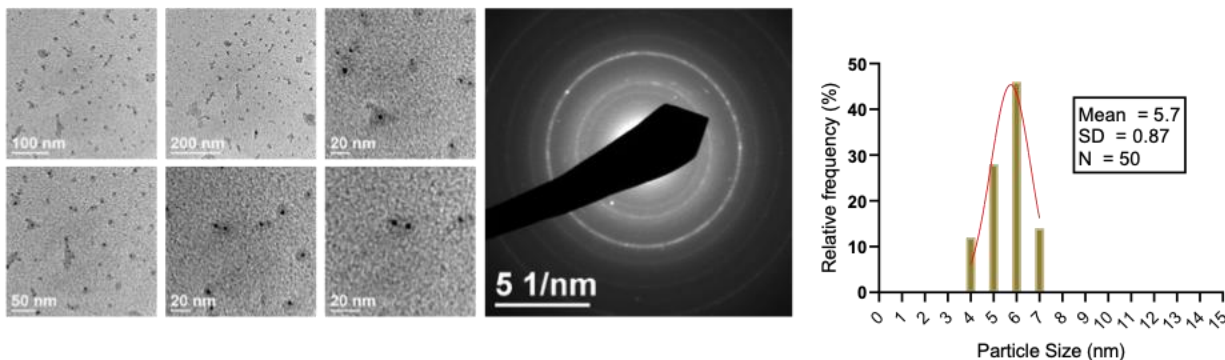


**Figure 8. TEM images, selected area electron diffraction pattern, and particle size distribution from image analysis for biosynthesized yttrium sulfide NPs.**

### 4.3 Task 3. Engineer rational control of PNCP biosynthesis and properties

#### Task 3.1: Generate *E. coli* strain producing both fluoride and metal-binding proteins/biomolecules.

We generated genetically modified *E. coli* using multiple strategies. One of them was to express each metal binding protein inside *E. coli* using a fluoride accumulating strain ( $\Delta$ *crcB*) and a non-fluoride accumulating strain (BL21(DE3)). Subsequently, we expressed the metal binding protein outside the cell using an outer membrane protein (OMP) fused to the metal binding protein, as illustrated in Figure 9.

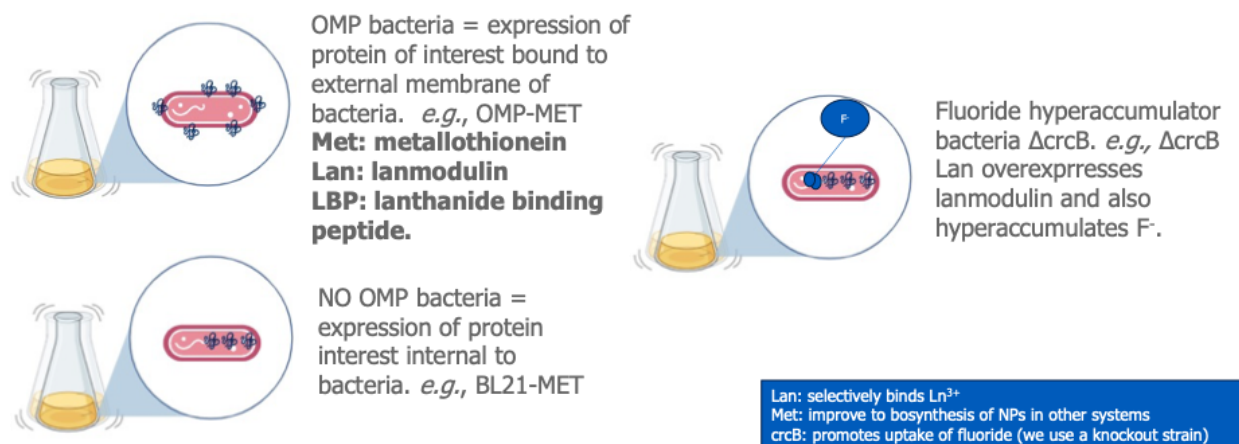
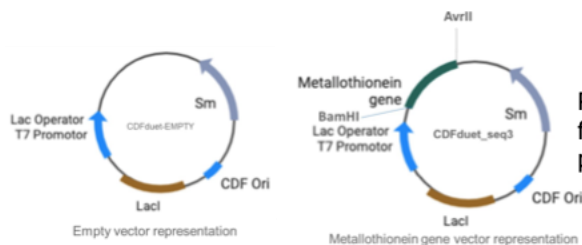


**Figure 9. Schematic illustration of strategies employed for genetic modification of *E. coli*.**

Figure 10 provides a schematic illustration of the strategy used to introduce the genetic modifications in *E. coli*, followed by a partial list of the plasmids and proteins that were expressed in *E. coli* for this project.

Metal-binding proteins were identified based upon literature reports and prior examples of nanoparticle production



Representative methodology for introducing metal-binding protein expression

Partial list of plasmids and proteins expressed in *E. coli* for this project.

Plasmid	Base Plasmid	Encoded Protein
Seq1(Strep <sup>R</sup> )	pCDFDuet-1	Gamma-glutamylcysteine synthetase from <i>Schizosaccharomyces pombe</i>
Seq2(Amp <sup>R</sup> )	pET14b	Phytochelatin synthetase from <i>Schizosaccharomyces pombe</i>
Seq3(Strep <sup>R</sup> )	pCDFDuet-1	Metallothionein from <i>Pseudomonas putida</i>
Seq4(Amp <sup>R</sup> )	pET14b	Phytochelatin synthase from <i>Arabidopsis thaliana</i>
Seq6(Amp <sup>R</sup> )	pET14b	Lanmodulin (LanM) from <i>Methylobacterium extorquens</i>
Seq7(Amp <sup>R</sup> )	pET14b	LutH from <i>Methylobacterium extorquens</i>
Seq6&7(Amp <sup>R</sup> )	pCDFDuet-1	Combined LanM and LutH
Seq10(Amp <sup>R</sup> )	pCDFDuet-1	Metallothionein linked to outer membrane protein A (OmpA)
Seq11(Amp <sup>R</sup> )	pET14b	Lanmodulin linked to OmpA

**Figure 10. Illustration of methodology used to introduce metal-binding protein expression and summary list of plasmids and proteins expressed in *E. coli* for this project.**

All these genetically modified bacteria were used in the REE-based NP biosynthesis through each protocol designed by our group.

**Task 3.5: Synthesize chemically and characterize NaYF<sub>4</sub>:REE.** Representative TEM images of chemically-synthesized NPs of cubic and hexagonal NaYF<sub>4</sub> are shown in Figure 11(A-C). These are the expected structures and crystal phases, with the expected bright upconverted luminescence. Representative XRD patterns confirming the crystal phase of each NP type are provided in Figure 11(D,E). We have not pursued these further, as we focused on developing the biosynthesis routes.

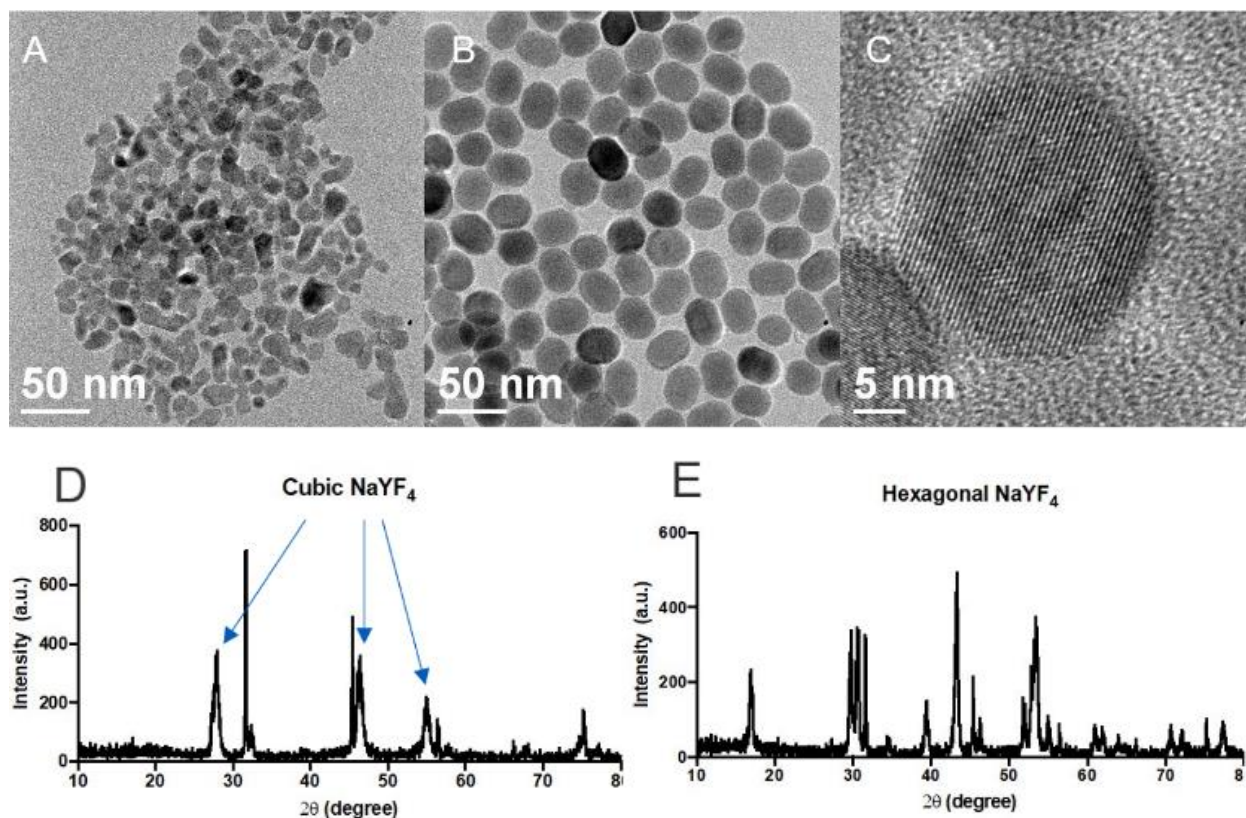


**Figure 11. TEM images of chemically synthesized NaYF<sub>4</sub> NPs. A) cubic and B) hexagonal phase NaYF<sub>4</sub>. C) High resolution TEM image of hexagonal NaYF<sub>4</sub> NPs. XRD patterns of D) cubic phase and E) hexagonal phase NaYF<sub>4</sub> NPs. Sharp impurity peaks are salt (NaCl) residue.**

#### 4.4 Task 4. Produce and optimize more complex REE-containing NPs in *E. coli*

**Task 4.1: Biogenically generate core-shell NPs in *E. coli*.** This task was accomplished *via* biosynthesis of REE-sulfide nanoparticles with different REEs in the core and shell, as shown in Figure 12 for the prototypical example of TbS core particles coated with an yttrium-based shell. In this example, the TbS synthesis proceeded as usual except that after 30 minutes of synthesis, yttrium nitrate was added, leading to the formation of an yttrium-rich shell.

In addition to core-shell structures, we found that doping of TbS NPs could dramatically increase the quantum yield for downconversion emission. This was measured using an integrating sphere apparatus to achieve absolute measurements of photons absorbed and emitted, as illustrated in the left panel of Figure 13.

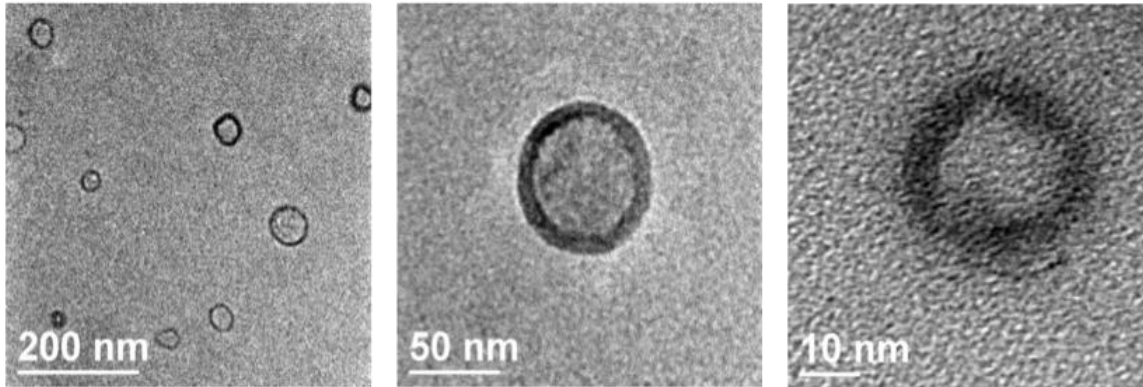
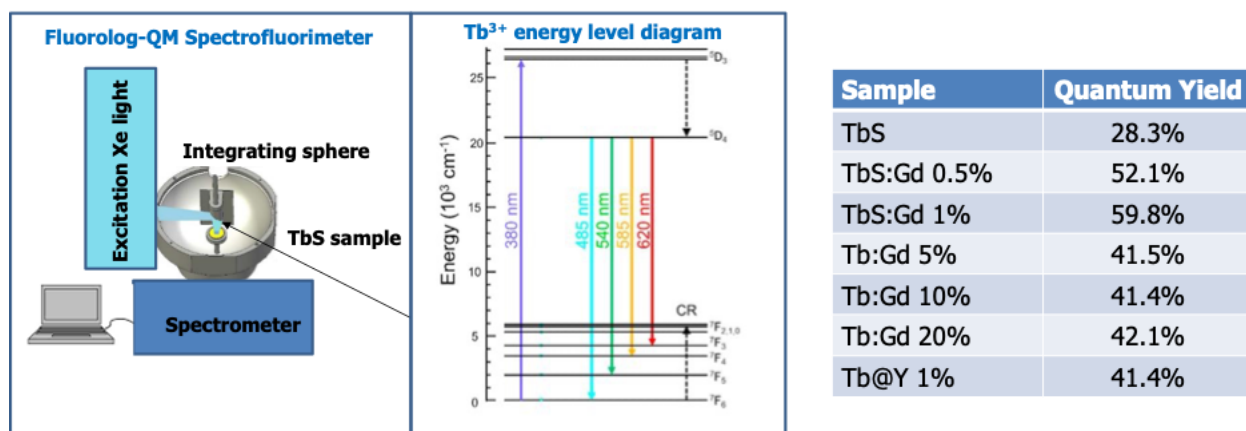


Figure 12. Representative TEM images of TbS core/YS shell nanoparticles.



Both doping with Gd (Tb:Gd) and deposition of a Y-rich shell (Tb@Y) lead to substantial increase in QY

Figure 13. Illustration of integrating sphere configuration used for measurement of quantum yield (QY) of downconverted emission from 390 nm to the wavelengths indicated in the energy level diagram. As tabulated in the accompanying table, the QY of TbS emission was dramatically enhanced by doping with Gd and by coating with an yttrium-rich shell.

## 5. Conclusion

The results presented above, along with the much more detailed results presented in monthly meetings and reports, demonstrate that all project milestones were achieved. Most importantly, the final project goal of producing  $\geq 2$  REE-containing biogenic PCNPs with downconversion quantum efficiency (QE) exceeding 25% along with  $>200$  nm Stokes shift was substantially exceeded by the REE sulfide materials shown in Figure 13. The first demonstrations of biogenic synthesis of upconverting rare-earth fluoride nanoparticles, using both wild-type and genetically-modified bacteria, was another key breakthrough of this project. These results demonstrate that microbial synthesis at near-ambient conditions can produce REE containing NPs with useful optical properties, and in the case of rare-earth sulfides, can produce materials that are difficult or impossible to access by other means. Further investment would be required to optimize and scale up the processes for producing rare-earth sulfides and to probe the exploit the mechanisms of rare-earth fluoride synthesis.

## 6. References

- (1) Chen, J.; Zhao, J. X. Upconversion Nanomaterials: Synthesis, Mechanism, and Applications in Sensing. *Sensors (Basel, Switzerland)* **2012**, *12* (3), 2414. <https://doi.org/10.3390/S120302414>.
- (2) Chen, G.; Qiu, H.; Prasad, P. N.; Chen, X. Upconversion Nanoparticles: Design, Nanochemistry, and Applications in Theranostics. *Chemical Reviews* **2014**, *114* (10), 5161–5214. <https://doi.org/10.1021/cr400425h>.
- (3) Jiang, W.; Yi, J.; Li, X.; He, F.; Niu, N.; Chen, L. A Comprehensive Review on Upconversion Nanomaterials-Based Fluorescent Sensor for Environment, Biology, Food and Medicine Applications. *Biosensors* **2022**, *12* (11). <https://doi.org/10.3390/bios12111036>.
- (4) Tang, H.; Tao, W.; Zhu, B.; Wang, C.; Scarpa, F. Enhanced Upconversion Luminescence in NaYF<sub>4</sub>:Yb, Er Nanoparticles by Using Graphitic Carbon Shells. *Materials Research Express* **2019**, *6* (4), 045040. <https://doi.org/10.1088/2053-1591/aafb5>.
- (5) Rabouw, F. T.; Prins, P. T.; Villanueva-Delgado, P.; Castelijns, M.; Geitenbeek, R. G.; Meijerink, A. Quenching Pathways in NaYF<sub>4</sub>:Er<sup>3+</sup>, Yb<sup>3+</sup> Upconversion Nanocrystals. *ACS Nano* **2018**, *12* (5), 4812–4823. <https://doi.org/10.1021/acsnano.8b01545>.
- (6) Anderson, R. B.; Smith, S. J.; May, P. S.; Berry, M. T. Revisiting the NIR-to-Visible Upconversion Mechanism in  $\beta$ -NaYF<sub>4</sub>:Yb<sup>3+</sup>,Er<sup>3+</sup>. *Journal of Physical Chemistry Letters* **2014**, *5* (1), 36–42. [https://doi.org/10.1021/JZ402366R/SUPPL\\_FILE/JZ402366R\\_SI\\_001.PDF](https://doi.org/10.1021/JZ402366R/SUPPL_FILE/JZ402366R_SI_001.PDF).
- (7) Zhu, X.; Su, Q.; Feng, W.; Li, F. Anti-Stokes Shift Luminescent Materials for Bio-Applications. *Chemical Society Reviews* **2017**, *46* (4), 1025–1039. <https://doi.org/10.1039/c6cs00415f>.
- (8) Haase, M.; Schäfer, H. Upconverting Nanoparticles. *Angewandte Chemie International Edition* **2011**, *50* (26), 5808–5829. <https://doi.org/10.1002/ANIE.201005159>.
- (9) Arai, M. S.; de Camargo, A. S. S. Exploring the Use of Upconversion Nanoparticles in Chemical and Biological Sensors: From Surface Modifications to Point-of-Care Devices. *Nanoscale Advances* **2021**, *3* (18), 5135–5165. <https://doi.org/10.1039/d1na00327e>.
- (10) Liu, Y.; Lu, Y.; Yang, X.; Zheng, X.; Wen, S.; Wang, F.; Vidal, X.; Zhao, J.; Liu, D.; Zhou, Z.; Ma, C.; Zhou, J.; Piper, J. A.; Xi, P.; Jin, D. Amplified Stimulated Emission in Upconversion Nanoparticles for Super-Resolution Nanoscopy. *Nature* **2017**, *543* (7644), 229–233. <https://doi.org/10.1038/nature21366>.
- (11) Ghazy, A.; Safdar, M.; Lastusaari, M.; Savin, H.; Karppinen, M. Advances in Upconversion Enhanced Solar Cell Performance. *Solar Energy Materials and Solar Cells* **2021**, *230* (April), 111234. <https://doi.org/10.1016/j.solmat.2021.111234>.
- (12) Krishnan, R.; Swart, H. C. Upconversion Luminescence Materials for Latent Fingerprint Detection Applications in Forensic Science. *Springer Nature Singapor* **2023**, No. August, 465–489. [https://doi.org/10.1007/978-981-99-3913-8\\_17](https://doi.org/10.1007/978-981-99-3913-8_17).
- (13) Matsubara, T.; Yamashita, T. Remote Optogenetics Using Up/Down-Conversion Phosphors. *Frontiers in Molecular Biosciences* **2021**, *8* (November), 1–10. <https://doi.org/10.3389/fmolb.2021.771717>.
- (14) Pliss, A.; Ohulchanskyy, T. Y.; Chen, G.; Damasco, J.; Bass, C. E.; Prasad, P. N. Subcellular Optogenetics Enacted by Targeted Nanotransformers of Near-Infrared Light. *ACS Photonics* **2017**, *4* (4), 806–814.

[https://doi.org/10.1021/ACSPHOTONICS.6B00475/SUPPL\\_FILE/PH6B00475\\_SI\\_001.PDF](https://doi.org/10.1021/ACSPHOTONICS.6B00475/SUPPL_FILE/PH6B00475_SI_001.PDF).

- (15) Jethva, P.; Momin, M.; Khan, T.; Omri, A. Lanthanide-Doped Upconversion Luminescent Nanoparticles—Evolving Role in Bioimaging, Biosensing, and Drug Delivery. *Materials* **2022**, *15* (7). <https://doi.org/10.3390/ma15072374>.
- (16) Alexaki, K.; Giust, D.; Kyriazi, M. E.; El-Sagheer, A. H.; Brown, T.; Muskens, O. L.; Kanaras, A. G. A DNA Sensor Based on Upconversion Nanoparticles and Two-Dimensional Dichalcogenide Materials. *Frontiers of Chemical Science and Engineering* **2021**, *15* (4), 935–943. <https://doi.org/10.1007/s11705-020-2023-9>.
- (17) Tao, K.; Sun, K. *Upconversion Nanoparticles: A Toolbox for Biomedical Applications*; Elsevier Inc., 2020.
- (18) Ghosh, S.; Ahmad, R.; Zeyauallah, M.; Khare, S. K. Microbial Nano-Factories: Synthesis and Biomedical Applications. *Frontiers in Chemistry* **2021**, *9*. <https://doi.org/10.3389/fchem.2021.626834>.
- (19) Bahrulolum, H.; Nooraei, S.; Javanshir, N.; Tarrhimofrad, H.; Mirbagheri, V. S.; Easton, A. J.; Ahmadian, G. Green Synthesis of Metal Nanoparticles Using Microorganisms and Their Application in the Agrifood Sector. *Journal of Nanobiotechnology* **2021**, *19* (1), 1–26. <https://doi.org/10.1186/s12951-021-00834-3>.
- (20) Vijayakumar, S.; Chen, J.; Amarnath, M.; Tungare, K.; Bhoori, M.; Divya, M.; González-Sánchez, Z. I.; Durán-Lara, E. F.; Vaseeharan, B. Cytotoxicity, Phytotoxicity, and Photocatalytic Assessment of Biopolymer Cellulose-Mediated Silver Nanoparticles. *Colloids and Surfaces A: Physicochemical and Engineering Aspects* **2021**, *628*, 127270. <https://doi.org/10.1016/J.COLSURFA.2021.127270>.
- (21) Pandit, C.; Roy, A.; Ghotekar, S.; Khusro, A.; Islam, M. N.; Bin Emran, T.; Lam, S. E.; Uddin Khandaker, M.; Bradley, D. A. Biological Agents for Synthesis of Nanoparticles and Their Applications. <https://doi.org/10.1016/j.jksus.2022.101869>.
- (22) Rajput, V. D.; Minkina, T.; Kimber, R. L.; Singh, V. K.; Shende, S.; Behal, A.; Sushkova, S.; Mandzhieva, S.; Lloyd, J. R. Insights into the Biosynthesis of Nanoparticles by the Genus *Shewanella*. *Applied and Environmental Microbiology* **2021**, *87* (22). <https://doi.org/10.1128/AEM.01390-21>.
- (23) Lucas, J.; Lucas, P.; Mercier, T. L.; Rollat, A.; Davenport, W. *Rare Earths Rare Earths Production and Use*; 2014.
- (24) Bonificio, W. D.; Clarke, D. R. Rare-Earth Separation Using Bacteria. *Environmental Science and Technology Letters* **2016**, *3* (4), 180–184. <https://doi.org/10.1021/acs.estlett.6b00064>.
- (25) Medin, S.; Schmitz, A. M.; Pian, B.; Mini, K.; Reid, M. C.; Holycross, M.; Gazel, E.; Wu, M.; Barstow, B. Genomic Characterization of Rare Earth Binding by *Shewanella Oneidensis*. *Scientific Reports* **2023**, *13* (1), 1–20. <https://doi.org/10.1038/s41598-023-42742-6>.
- (26) Plaza, D. O.; Gallardo, C.; Straub, Y. D.; Bravo, D.; Pérez-Donoso, J. M. Biological Synthesis of Fluorescent Nanoparticles by Cadmium and Tellurite Resistant Antarctic Bacteria: Exploring Novel Natural Nanofactories. *Microbial Cell Factories* **2016**, *15* (1), 76. <https://doi.org/10.1186/s12934-016-0477-8>.
- (27) Gallardo, C.; Monrás, J. P.; Plaza, D. O.; Collao, B.; Saona, L. A.; Durán-Toro, V.; Venegas, F. A.; Soto, C.; Ulloa, G.; Vásquez, C. C.; Bravo, D.; Pérez-Donoso, J. M. Low-Temperature Biosynthesis of Fluorescent Semiconductor Nanoparticles (CdS) by Oxidative

- Stress Resistant Antarctic Bacteria. *Journal of Biotechnology* **2014**, *187*, 108–115.  
<https://doi.org/10.1016/j.jbiotec.2014.07.017>.
- (28) Bao, G.; Wen, S.; Lin, G.; Yuan, J.; Lin, J.; Wong, K.-L.; Bünzli, J.-C. G.; Jin, D. Learning from Lanthanide Complexes: The Development of Dye-Lanthanide Nanoparticles and Their Biomedical Applications. *Coordination Chemistry Reviews* **2021**, *429*, 213642.  
<https://doi.org/10.1016/j.ccr.2020.213642>.
- (29) Duchna, M.; Cieřlik, I. Rare Earth Elements in New Advanced Engineering Applications. In *Rare Earth Elements - Emerging Advances, Technology Utilization, and Resource Procurement*; T. Aide, M., Ed.; IntechOpen, 2023.  
<https://doi.org/10.5772/intechopen.109248>.
- (30) Fan, Q.; Cui, X.; Guo, H.; Xu, Y.; Zhang, G.; Peng, B. Application of Rare Earth-Doped Nanoparticles in Biological Imaging and Tumor Treatment. *J Biomater Appl* **2020**, *35* (2), 237–263. <https://doi.org/10.1177/0885328220924540>.
- (31) Blasse, G. Chapter 34 Chemistry and Physics of R-Activated Phosphors. In *Handbook on the Physics and Chemistry of Rare Earths*; Elsevier, 1979; Vol. 4, pp 237–274.  
[https://doi.org/10.1016/S0168-1273\(79\)04007-1](https://doi.org/10.1016/S0168-1273(79)04007-1).
- (32) Yuan, J.; Wang, G. Lanthanide-Based Luminescence Probes and Time-Resolved Luminescence Bioassays. *TrAC Trends in Analytical Chemistry* **2006**, *25* (5), 490–500.  
<https://doi.org/10.1016/j.trac.2005.11.013>.
- (33) Kusriani, E.; Safira, A. I.; Usman, A.; Prasetyanto, E. A.; Nugrahaningtyas, K. D.; Santosa, S. J.; Wilson, L. D. Nanocomposites of Terbium Sulfide Nanoparticles with a Chitosan Capping Agent for Antibacterial Applications. *J. Compos. Sci.* **2023**, *7* (1), 39.  
<https://doi.org/10.3390/jcs7010039>.
- (34) Chen, Y.; Chi, Y.; Wen, H.; Lu, Z. Sensitized Luminescent Terbium Nanoparticles: Preparation and Time-Resolved Fluorescence Assay for DNA. *Anal. Chem.* **2007**, *79* (3), 960–965. <https://doi.org/10.1021/ac061477h>.
- (35) Charpentier, C.; Cifliku, V.; Goetz, J.; Nonat, A.; Cheignon, C.; Cardoso Dos Santos, M.; Francés-Soriano, L.; Wong, K.; Charbonnière, L. J.; Hildebrandt, N. Ultrabright Terbium Nanoparticles for FRET Biosensing and in Situ Imaging of Epidermal Growth Factor Receptors\*\*. *Chemistry A European J* **2020**, *26* (64), 14602–14611.  
<https://doi.org/10.1002/chem.202002007>.
- (36) Lai, C.-H.; Lu, M.-Y.; Chen, L.-J. Metal Sulfide Nanostructures: Synthesis, Properties and Applications in Energy Conversion and Storage. *J. Mater. Chem.* **2012**, *22* (1), 19–30.  
<https://doi.org/10.1039/C1JM13879K>.
- (37) Fei, W.; Zhang, M.; Fan, X.; Ye, Y.; Zhao, M.; Zheng, C.; Li, Y.; Zheng, X. Engineering of Bioactive Metal Sulfide Nanomaterials for Cancer Therapy. *J Nanobiotechnol* **2021**, *19* (1), 93. <https://doi.org/10.1186/s12951-021-00839-y>.
- (38) Tiseanu, C.; Mehra, R. K.; Kho, R.; Kumke, M. Comparative Study of Time-Resolved Photoluminescence Properties of Terbium-Doped Thiosalicylic-Capped CdS and ZnS Nanocrystals. *J. Phys. Chem. B* **2003**, *107* (44), 12153–12160.  
<https://doi.org/10.1021/jp035322e>.
- (39) Tiseanu, C.; Mehra, R. K.; Kho, R. Optical Response of Thiosalicylic-Capped CdS Nanocrystals to Terbium Ions. *Journal of Photochemistry and Photobiology A: Chemistry* **2005**, *173* (2), 169–173. <https://doi.org/10.1016/j.jphotochem.2005.01.017>.
- (40) Debnath, G. H.; Chakraborty, A.; Ghatak, A.; Mandal, M.; Mukherjee, P. Controlled Terbium(III) Luminescence in Zinc Sulfide Nanoparticles: An Assessment of Competitive

- Photophysical Processes. *J. Phys. Chem. C* **2015**, *119* (42), 24132–24141. <https://doi.org/10.1021/acs.jpcc.5b07182>.
- (41) Poornaprakash, B.; Chalapathi, U.; Suh, Y.; Vattikuti, S. V. P.; Reddy, M. S. P.; Park, S.-H. Terbium-Doped ZnS Quantum Dots: Structural, Morphological, Optical, Photoluminescence, and Photocatalytic Properties. *Ceramics International* **2018**, *44* (10), 11724–11729. <https://doi.org/10.1016/j.ceramint.2018.03.250>.
- (42) Shkir, Mohd.; Chandekar, K. V.; Alshahrani, T.; Kumar, A.; AlFaify, S. A Novel Terbium Doping Effect on Physical Properties of Lead Sulfide Nanostructures: A Facile Synthesis and Characterization. *J. Mater. Res.* **2020**, *35* (20), 2664–2675. <https://doi.org/10.1557/jmr.2020.216>.
- (43) Fu, J.; Wang, L.; Chen, H.; Bo, L.; Zhou, C.; Chen, J. A Selective Fluorescence Probe for Mercury Ion Based on the Fluorescence Quenching of Terbium(III)-Doped Cadmium Sulfide Composite Nanoparticles. *Spectrochimica Acta Part A: Molecular and Biomolecular Spectroscopy* **2010**, *77* (3), 625–629. <https://doi.org/10.1016/j.saa.2010.06.038>.
- (44) Fitriyanto, N. A.; Fushimi, M.; Matsunaga, M.; Pertiwinigrum, A.; Iwama, T.; Kawai, K. Molecular Structure and Gene Analysis of Ce<sup>3+</sup>-Induced Methanol Dehydrogenase of Bradyrhizobium Sp. MAFF211645. *Journal of Bioscience and Bioengineering* **2011**, *111* (6), 613–617. <https://doi.org/10.1016/j.jbiosc.2011.01.015>.
- (45) Hibi, Y.; Asai, K.; Arafuka, H.; Hamajima, M.; Iwama, T.; Kawai, K. Molecular Structure of La<sup>3+</sup>-Induced Methanol Dehydrogenase-like Protein in Methylobacterium Radiotolerans. *Journal of Bioscience and Bioengineering* **2011**, *111* (5), 547–549. <https://doi.org/10.1016/j.jbiosc.2010.12.017>.
- (46) Nakagawa, T.; Mitsui, R.; Tani, A.; Sasa, K.; Tashiro, S.; Iwama, T.; Hayakawa, T.; Kawai, K. A Catalytic Role of XoxF1 as La<sup>3+</sup>-Dependent Methanol Dehydrogenase in Methylobacterium Exorquens Strain AM1. *PLoS ONE* **2012**, *7* (11), e50480. <https://doi.org/10.1371/journal.pone.0050480>.
- (47) Cotruvo, J. A.; Featherston, E. R.; Mattocks, J. A.; Ho, J. V.; Laremore, T. N. Lanmodulin: A Highly Selective Lanthanide-Binding Protein from a Lanthanide-Utilizing Bacterium. *J. Am. Chem. Soc.* **2018**, *140* (44), 15056–15061. <https://doi.org/10.1021/jacs.8b09842>.
- (48) Yang, Q.; Wang, L.; Zhou, Q.; Huang, X. Toxic Effects of Heavy Metal Terbium Ion on the Composition and Functions of Cell Membrane in Horseradish Roots. *Ecotoxicology and Environmental Safety* **2015**, *111*, 48–58. <https://doi.org/10.1016/j.ecoenv.2014.10.002>.
- (49) Jiang, N.; Wang, L.; Lu, T.; Huang, X. Toxic Effect of Terbium Ion on Horseradish Cell. *Biol Trace Elem Res* **2011**, *143* (3), 1722–1728. <https://doi.org/10.1007/s12011-011-8968-2>.
- (50) Rim, K. T.; Koo, K. H.; Park, J. S. Toxicological Evaluations of Rare Earths and Their Health Impacts to Workers: A Literature Review. *Safety and Health at Work* **2013**, *4* (1), 12–26. <https://doi.org/10.5491/SHAW.2013.4.1.12>.
- (51) Martínez Meroño, R. M. The Effect of Lanthanides and Their Nanoparticles on Pathogenic Bacteria, Universitat Politècnica de València, 2020.
- (52) Park, D. M.; Reed, D. W.; Yung, M. C.; Eslamimanesh, A.; Lencka, M. M.; Anderko, A.; Fujita, Y.; Riman, R. E.; Navrotsky, A.; Jiao, Y. Bioadsorption of Rare Earth Elements through Cell Surface Display of Lanthanide Binding Tags. *Environ. Sci. Technol.* **2016**, *50* (5), 2735–2742. <https://doi.org/10.1021/acs.est.5b06129>.

- (53) Brewer, A.; Chang, E.; Park, D. M.; Kou, T.; Li, Y.; Lammers, L. N.; Jiao, Y. Recovery of Rare Earth Elements from Geothermal Fluids through Bacterial Cell Surface Adsorption. *Environ. Sci. Technol.* **2019**, *53* (13), 7714–7723. <https://doi.org/10.1021/acs.est.9b00301>.
- (54) Iram, S.; Khan, S.; Ansary, A. A.; Arshad, M.; Siddiqui, S.; Ahmad, E.; Khan, R. H.; Khan, M. S. Biogenic Terbium Oxide Nanoparticles as the Vanguard against Osteosarcoma. *Spectrochimica Acta Part A: Molecular and Biomolecular Spectroscopy* **2016**, *168*, 123–131. <https://doi.org/10.1016/j.saa.2016.05.053>.

## **Appendix 1. Project Coordination, Dissemination, and Translation Efforts**

### **Project Coordination**

Describe who was part of your project's team and what their contributions were:

PI: Paras Prasad, coordinated overall project and led research team.

co-PI: Blaine Pfeifer, oversaw all bioengineering aspects of the project

co-PI: Mark Swihart, oversaw all nanomaterial characterization and chemical and hydrothermal synthesis of nanoparticles.

Key collaborator: José Manuel Pérez-Donoso, advised on biosynthesis protocols and mentored post-doctoral and graduate student researchers.

#### Senior Personnel:

Dr. Alexander Baev, theoretical and computational support.

Dr. Andrey Kuzmin, spectroscopic characterization of materials.

#### Post-doctoral researcher:

Dr. Nia Oetiker, hands-on participation in all aspects of project, especially biosynthesis of REE-doped NaYF<sub>4</sub>

#### Graduate students:

Juan Jose Leon, visiting student from Chile, hands-on participation in biosynthesis, especially biosynthesis of REE sulfides.

Justin Bassett, genetic modification of *E. coli* and other bioengineering aspects.

Kaiwen Chen, chemical synthesis of REE-doped nanoparticles, nanomaterial characterization, hydrothermal synthesis and aqueous high-concentration biosynthesis of nanoparticles.

Note changes in key personnel (if any)

None

### **Summarize key trips, meetings, or conferences and provide the following:**

Bio-INC program review, April 2023

Bio-INC virtual program review, November 2023

**Dissemination and Translation (if applicable)**

We have no immediate plans for translation - this was a one-year exploratory project.

Results will be disseminated in roughly 6 publications, of which two are submitted or ready for submission, and the remainder are at varying degrees of preparation.

**Publications and Presentations**

Please update the table below with any current or upcoming publications. This section will be cumulative for your effort.

Title, Authors	Description/Type	Date Sent to DARPA/Agent	Status
Microbial Green Synthesis of Luminescent Terbium Sulfide Nanoparticles using <i>E. coli</i>	Submitted to <i>Journal of Nanobiotechnology</i>		submitted
Biosynthesis of Up-converting Luminescent Nanoparticles by Antarctic <i>Shewanella</i> Bacteria	To be submitted		In preparation

An acknowledgement of the Government's support in any scientific publication developed under your contract/grant must be included.

## Appendix 2. Schedule: Milestones and Deliverables

Provide a readable, high-level Gantt chart for the project that lists the major milestones and deliverables for each Task. Use month and year to label your chart, for example, Mar-22. You may attach the Gantt chart as a separate document. Tasks: Progress, Accomplishments, and Plans

**Table 2-2. Summary of Tasks and Completion Dates**

	Task	Date
Task 1 (UB)	Doping CdS NPs with REEs in <i>E. coli</i> .	Nov. 2022
1.1	Produce CdS QDs in <i>E. coli</i>	Nov. 2022
1.2	Dope CdS QDs with REEs in <i>E. coli</i>	Dec. 2022
Milestone	Demonstrate bio-based incorporation of REE in an inorganic nanoparticle for $\geq 2$ different REEs	Jan. 2023
1.3	Optically characterize REE-doped NPs	Jan. 2023
Milestone	Demonstrate a biogenic nanoparticle composition that exhibits downconverted luminescence.	Dec. 2022
1.4	Synthesize chemically and characterize CdS:REE QDs	Jan. 2023
Task 2 (UB)	Biosynthesis of REE-doped NaYF <sub>4</sub> NPs in bacteria	Apr. 2023
2.1	Generate an <i>E. coli</i> strain producing high levels of fluoride intracellularly	Nov. 2023
2.2	Synthesize NaYF <sub>4</sub> NPs in recombinant <i>E. coli</i> strain	Nov. 2023
Mile-stone	Bio-based production of similarly sized nanoparticles (50 nm width)	Apr. 2023
2.3	Dope NaYF <sub>4</sub> NPs with Er <sup>3+</sup> ions	Apr. 2023
2.4	Co-dope NaYF <sub>4</sub> : Er <sup>3+</sup> NPs with Nd <sup>3+</sup> and/or Yb <sup>3+</sup> ions; create core/shell or surface modified PCNPs	Apr. 2023
2.5	Synthesize chemically and characterize NaYF <sub>4</sub> :REE	May 2023

Milestone	Produce $\geq 5$ distinct nanoparticle compositions that downconvert light with Stokes shift $> 50$ nm	July 2023
Task 3 (UB)	Engineer rational control of PNCP biosynthesis and properties	July 2023
3.1	Generate <i>E. coli</i> strain producing both fluoride and metal-binding proteins/biomolecules	Oct. 2023
3.2	Control NaYF <sub>4</sub> :REE by genetically modifying <i>E. coli</i>	Nov. 2023
3.3	Control NaYF <sub>4</sub> :REE by modifying the reaction conditions	Nov. 2023
3.5	Synthesize chemically and characterize NaYF <sub>4</sub> :REE	Dec. 2022
Milestones	Demonstrate interchangeable incorporation of $>3$ REE; Achieve at least 1 formulation with $>15\%$ QE and $>100$ nm Stokes shift	Oct. 2023
Task 4 (UB)	Produce and optimize more complex REE-containing NPs in <i>E. coli</i>	Dec. 2023
4.1	Biogenically generate core-shell NPs in <i>E. coli</i>	Aug. 2023
4.2	Generate core-shell NPs by cation exchange process	N/A
Milestone	Produce nanoparticles with performance-enhancing surface layer ( $>20\%$ thickness variation)	Oct. 2023
4.3	Synthesize chemically and characterize NaYF <sub>4</sub> :REE PCNPs	Nov. 2023
Mile-stone	Change vis/NIR absorbance/emission by changing REE stoichiometry	
Milestone	Provide status report comparing attributes and limitations of biogenic and conventionally-prepared PCNPs	Sept. 2023
Milestone	Demonstrate size control of REE-doped core-shell PCNPs, 5 to 30 nm diameter, $<10$ nm variation, size-dependent optical properties	Nov. 2023
Final goal	Demonstrate $\geq 2$ REE-containing biogenic PCNPs with $< 50$ nm emission FWHM, $>25\%$ QE, and $>200$ nm Stokes shift; final report	Nov. 2023

## **LIST OF SYMBOLS, ABBREVIATIONS, AND ACRONYMS**

AFRL	Air Force Research laboratory
EDS	Energy-Dispersive X-ray Spectroscopy
NP	Nanoparticle
REE	Rare-earth element
RXEB	Biomaterials Branch, Photonic, Electronic, and Soft Materials Division, Materials and Manufacturing Directorate
SAED	Selected Area Electron Diffraction
STEM	Scanning Transmission Electron Microscopy
TEM	Transmission Electron Microscopy
UCNP	Upconverting Nanoparticle
WPAFB	Wright-Patterson Air Force Base
XRD	X-ray Diffraction